

Received January 15, 2019, accepted February 20, 2019, date of publication February 25, 2019, date of current version March 18, 2019.

Digital Object Identifier 10.1109/ACCESS.2019.2901446

# Design of a Polarization-Diverse Planar Leaky-Wave Antenna for Broadside Radiation

DAVIDE COMITE<sup>1</sup>, (Member, IEEE), SYMON K. PODILCHAK<sup>2</sup>, (Member, IEEE),  
PAOLO BACCARELLI<sup>3</sup>, (Member, IEEE), PAOLO BURGHIGNOLI<sup>1</sup>, (Senior Member, IEEE),  
ALESSANDRO GALLI<sup>1</sup>, (Member, IEEE), ALOIS P. FREUNDORFER<sup>4</sup>, (Senior Member, IEEE),  
AND YAHIA M. M. ANTAR<sup>4</sup>, (Life Fellow, IEEE)

<sup>1</sup>Department of Information Engineering, Electronics and Telecommunications, Sapienza University of Rome, 00184 Rome, Italy

<sup>2</sup>School of Engineering and Physical Sciences Edinburgh Campus, Institute of Sensors, Signals, and Systems, Heriot-Watt University, Edinburgh EH14 4AS, U.K.

<sup>3</sup>Department of Engineering, Roma Tre University, 00146 Rome, Italy

<sup>4</sup>Department of Electrical and Computer Engineering, Royal Military College of Canada, Kingston, ON K7K 7B4, Canada

Corresponding author: Davide Comite (davide.comite@uniroma1.it)

This work was supported by the European Union's Horizon 2020 Research and Innovation Programme under the Marie Skłodowska-Curie Project CSA-EU under Grant 709372.

**ABSTRACT** The design of a K-band radial leaky-wave antenna is presented for polarization diversity applications. The antenna structure is constituted by an annular, radially periodic, and metallic strip grating printed on top of a single-layer grounded dielectric slab. The integrated feeding system is defined by a  $2 \times 2$  array of planar slot sources for cylindrical surface-wave excitation. By the addition of the grating, the surface wave is perturbed and enables cylindrical leaky-wave radiation by means of a fast  $n = -1$  space harmonic, whose behavior is characterized through a full-wave dispersive analysis. By proper phasing and spacing of the four independent TM feeds, positioned close to the center of the annular grating and on the ground plane, we demonstrate the possibility of radiating directive broadside beams offering linear, left- or right-handed circularly polarized radiation, and sum and delta patterns. Thus, we propose an original solution to flexibly control the polarization of a high-gain beam by means of a simple and low-cost feeding system, made by the minimum number of integrated array sources. To accurately assess the antenna features and performance, the role of a zeroth- and first-order cylindrical leaky waves propagating along the antenna aperture is also discussed. The proposed antenna design may be of interest for direction-of-arrival estimation by means of monopulse radars, as well as for a wide class of applications where flexible control of the polarization is desired, such as satellite and terrestrial point-to-point communication systems and earth observation.

**INDEX TERMS** Leaky-wave antenna, surface wave, circular polarization, dual polarization, antenna arrays, monopulse radar, remote sensing.

## I. INTRODUCTION AND BACKGROUND

Modern radar and communication systems call for the design of low-cost and low-profile antenna designs with polarization-reconfigurability of the far-field pattern. The most common solution to achieve this functionality consists in the design of two-dimensional (2-D) arrays of microstrip patches, properly excited by means of integrated feeding networks [1]. As is well known, this class of antenna can present design challenges, especially in the microwave and millimeter-wave frequency regions, where radiation

efficiencies may become low due to unwanted surface-wave (SW) excitations on the antenna aperture.

To obtain circular polarized (CP) far-field beam patterns, for example, arrays of linearly polarized (LP) elements can be considered [2], [3]. This can be composed of microstrip patches or horn antennas, and should be arranged in a  $5 \times 5$  (or more) array of square elements to achieve high directivity. However, at microwave and millimeter-wave frequencies, these conventional solutions can become very challenging to design, manufacture, and integrate, possibly requiring bulky and corporate feed systems which can also reduce the realized antenna gain. In addition, SW fields can become problematic. In this frame, due to their low-profile and planar nature,

The associate editor coordinating the review of this manuscript and approving it for publication was Mengmeng Li.

Fabry-Perot cavity antennas (FPCAs) [4] have been proposed as a very good alternative to generate LP or CP pencil beams with medium or high realized gain values, and numerous solutions have been reported in the last few decades (see, e.g., [5]–[10] and references therein).

An alternative solution to synthesize CP or LP beam patterns by means of printed and low-cost structures can be one-dimensional (1-D) and two-dimensional (2-D) leaky-wave antennas (LWAs) [11]. Different designs have been proposed in the last few decades offering CP radiation [12]–[17]. They typically make use of single feeding points and of suitably-designed unit cells, which can also be arranged in a clever double-layer configuration to achieve dual-polarized operation [18]. Other polarization-diverse or reconfigurable antennas may also be of interest that can offer sum and difference patterns for radar and direction-of-arrival estimation. For example, monopulse antennas can be designed using parabolic or lens-based configurations, which can become very complicated, expensive, and heavy [1]. Several alternatives have been proposed based on radial-line slotted arrays [19], [20], planar microstrip arrays [21], substrate integrated waveguide technology [22], [23], FPCAs [24], holographic LWAs [25], and gap waveguide technology [26].

An attractive simple and low-cost solution to synthesize high-gain LP and CP beams as well as monopulse patterns, with the same antenna structure, can be made possible by array-fed 2-D LWAs. This is proposed here through the excitation of a fast space harmonic [11], achieved by periodically perturbing the fundamental surface wave (SW) supported by a grounded dielectric slab (GDS), and feeding the antenna by introducing a small number of fully-integrated phased sources, while expanding on the originally studied in [27], [28], and [29] which mainly investigated single-frequency beam steering at broadside.

In general, by loading the top layer of the employed GDS by means of any sort of perturbation mechanism, the transformation of the guided SW into a fast wave is made possible such that power is leaked along the air-dielectric interface for radiation. This can be accomplished by considering an annular arrangement of microstrip lines; i.e., a radially periodic bull-eye LWA, with azimuthal symmetry, defining a metallic strip grating (MSG) configuration [30]–[33]. Depending on the source and on the operational frequency, 2-D planar LWAs can enable radiation with directive frequency-scanning patterns as well as broadside pencil beams.

On this basis, simple and efficient antenna feeding can be made possible using an arrangement of slots in the ground plane of the employed GDS for SW excitation. This is in contrast to more conventional planar phased array design approaches, which, instead, aim to suppress such slow, guided-waves. When considering relatively high-dielectric constant values, efficient TM SW excitation has been shown by means of planar surface-wave launchers (SWLs) [34], [35]. In particular, this SW source can act as a printed magnetic dipole element and both directive and

non-directive SWLs have been proposed for the realization of unidirectional and bi-directional TM SW field distributions [31], [36], [37], with an original  $2 \times 2$  SWL array reported in [27].

To generate a highly directional beam using an array of such SW sources, the 2-D LWA has to be properly designed to support a weakly-attenuated cylindrical leaky wave (CLW) [38]; i.e., a traveling-wave having either no azimuthal variation on the aperture ( $m = 0$  modes) or with some azimuthal  $\phi$  dependence varying as  $\sin \phi$  or  $\cos \phi$  ( $m = 1$  modes). In both cases, the contribution to the aperture field should be made dominant with respect to other guided modes and to the space wave (see, e.g., [1, Ch. 7]). Depending on the geometric symmetry enforced by the feeder, CLWs can generate pencil or conical patterns in the far field [38]. For instance, if an LP or CP broadside pencil beam is desired, a single CLW of order  $m = 1$  or two in-quadrature CLWs of order  $m = 1$  with a mutual azimuthal shift of  $\pi/2$  are required, the latter resulting in a single CLW with an azimuthal dependence of the kind  $e^{\pm j\phi}$ .

To achieve such a polarization reconfigurability of the far-field beam pattern, we propose the design of an annular bull-eye LWA fed by non-directive SWLs whilst considering 50- $\Omega$  coplanar waveguide transmission-line connectivity [31], [37]. More specifically, we report the complete findings of an original  $2 \times 2$  square arrangement of non-directive SWLs [27] positioned at the origin of the ground plane (see Fig. 1) with LW radiation by the printed MSG on the top air-dielectric interface of the employed GDS.

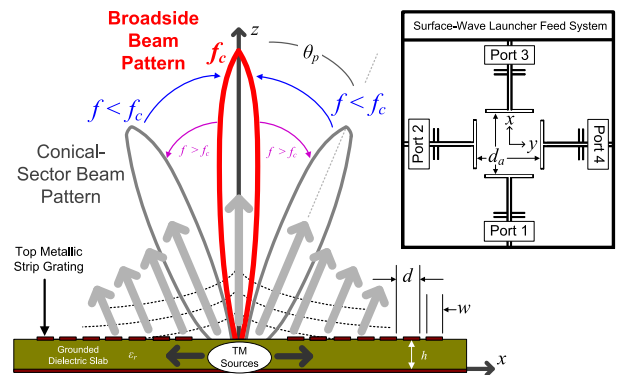


**FIGURE 1.** Cross-sectional view of the proposed LWA. Broadside radiation is possible at about  $f_c$  as well as a two-sided conical-sector beam pattern below and above  $f_c$  [1, Ch. 7]. The  $2 \times 2$  antenna source arrangement in the ground plane (see inset) can act as the planar feed for TM cylindrical-wave excitation offering both LP and CP as well as sum and difference patterns.

When the SWL elements for this feeding array are properly separated and phased, a polarization-reconfigurable 2-D LWA can be realized offering LP, left- or right-handed circularly polarized (LHCP or RHCP) radiation, as well as sum and difference LP monopulse far-field patterns. Moreover, when generally considering the frequency scanning characteristics of the proposed 2-D LWA and the particular SWL source implementation, as well as the defined magnitude

and relative phase difference between SW elements, conical beam patterns in the far-field that scan with frequency are possible [33], [39] as well as two-sided conical-sector beam patterns. To the best of the authors' knowledge no similar antenna structure, offering flexible control of the polarization through a  $2 \times 2$  arrangement of non-directional SWLs, has been theoretically analyzed and experimentally verified.

These antenna characteristics are particularly suitable for radar applications such as automotive and monopulse, as well as next-generation indoor wireless communication systems, which require the engineer to accommodate for multipath environments and to remove the need for any transmitter and receiver alignment. It is also of interest for applications oriented to the Global Navigation Satellite System (GNSS), and other satellite systems where polarization-dependent effects (such as rain clutter and Faraday rotation) have to be corrected and it can represent an attractive solution for earth observation based on compact polarimetry [40].

This paper is organized as follows. In Sect. II the modal analyses of the relevant SWs and LWs supported by the structure are discussed considering a linearized version of the radial aperture. Results are compared to a measured prototype considering a single SWL source. In Sects. III and IV, full-wave simulations and experimental validations of a measured planar LWA prototype are studied with the aforementioned  $2 \times 2$  SWL square array where LP, CP and sum/difference patterns are reported. Conclusions follow in Sect. V.

## II. DISPERSION ANALYSIS AND ANTENNA CHARACTERIZATION

Practical implementation of the polarization-diverse LWA with an integrated array-feed system can be challenging at microwave and millimeter-wave frequencies, especially a design which ensures efficient SW excitation. As presented here, a  $2 \times 2$  array of SW sources can represent a simple and effective means to achieve higher-order cylindrical  $\text{TM}_0$  SW excitation for LW radiation and polarization control of the far-field pattern. Indeed, polarization diversity can be made possible by properly tuning the relative magnitude and phase between these planar integrated sources in the ground plane.

The SWLs considered here represent an arrangement of magnetic dipole sources on the ground of a GDS made with a high value for the relative dielectric constant ( $\epsilon_r > 10$ ), and by substrates having thickness according to  $h\sqrt{\epsilon_r}/\lambda_0 \approx 1/4$  [31], they excite a bound  $\text{TM}_0$  mode whilst operating above the  $\text{TE}_1$  mode cutoff frequency. Typically, under these conditions more than 80% of the input power can be coupled into the dominant  $\text{TM}_0$  SW mode of the slab for radiation [27], [31]. Our reported array-fed, 2-D planar, LWA design is illustrated in Fig. 1. The square arrangement of SWLs in the ground plane, positioned at the origin is also shown in the relevant inset. The four-port (i.e.,  $2 \times 2$ ) feeder can excite a cylindrical SW perturbed by the top azimuthally symmetric bull-eye MSG.

The distance between elements is sized considering the phase constant  $\beta^{\text{TM}_0}$  of the  $\text{TM}_0$  surface wave of the GDS.

The MSG, indeed, is not homogenizable and, thus, it does not provide translational invariance. Therefore, since the four SWLs are not placed exactly in the center, each of them operates "seeing" a MSG not exactly azimuthally symmetric. However, by enforcing the condition  $d_a = \lambda_g/2$ , with  $\lambda_g = 2\pi/\beta^{\text{TM}_0}$  one gets a mutual distance  $d_a$  between opposite SWLs of 4.1 mm [27], which is further finely tuned to optimize the 50- $\Omega$  input impedance matching. This distance is small enough to keep the SWL array within the first annular ring of the MSG, and to let it constitute a good discrete approximation of a continuous, azimuthally directed, magnetic ring source concentric to the annular MSG.

### A. DISPERSIVE ANALYSIS

To characterize the modal features of the open waveguide, a dispersive analysis of the equivalent 1-D linearized (lossless) structure, i.e., the metal strip grating over a grounded dielectric slab (MSG-GDS), has been developed by using the MoM approach in [41] and [42], as was previously done for similar 2-D annular configurations in [30], [31], [37], [43], and [44], where a detailed discussion on these modeling aspects was provided considering both far- and near-field regimes.

The modal spectrum propagating along the linearized periodic structure can be divided into TM and TE modes, each mode being characterized by a Floquet representation in terms of an infinite number of space harmonics with wavenumbers defined by  $k_{\rho n} = \beta_0 + 2\pi n/d - j\alpha$  [11],  $d$  being the period of the grating. Typically, the radial LWA structure is optimized for radiation through the  $n = -1$  space harmonic [1, Ch. 7]. By properly designing the MSG, low attenuation rates can be obtained and directive beam patterns can be observed in the far-field (see, e.g., [31], [33], [37]).

The normalized dispersion curves of the LW phase and attenuation constants,  $\beta_{-1}$  and  $\alpha$ , versus frequency, for the LWA structure considered here are reported in Fig. 2. The substrate has permittivity  $\epsilon_r = 10.2$  and thickness  $h = 1.27$  mm (see Fig. 1). A further case, which stems by practical tolerancing considerations for the relative dielectric constant of the employed GDS, i.e.  $\epsilon_r = 11.5$ , as for the similar LWA structure (see Figs. 16 and 17 from [31]), is also considered. It can be observed that the  $n = -1$  space-harmonic phase constant for the considered LW mode increases almost linearly with frequency, changing its sign passing through broadside, i.e.,  $\beta_{-1}/k_0 = 0$ , at an open stop-band frequency value  $f_c$  equal to about 21.5 GHz [20.3 GHz] for  $\epsilon_r = 10.2$  [for  $\epsilon_r = 11.5$ ]. This defines a *proper* LW (i.e., for negative values of  $\beta_{-1}/k_0$ ) and an *improper* LW (i.e., for the positive ones) [1, Ch. 7].

Depending on the feed configuration and on the operating frequencies, the CLW supported by the corresponding 2-D LWA can generate a conical or conical-sector (two-sided) pattern in the far-field, with the main beam scanning with the frequency from backward endfire towards broadside ( $f < f_c$ ). With an increase in frequency and such that  $|\beta_{-1}| \leq \alpha$  (i.e., at the beam splitting condition [45]), the conical beam

coalesces into a single pencil beam radiating at broadside. Then for a continued increase of the frequency, the beam opens again ( $\beta_{-1} \geq \alpha$ ) and the resulting conical or conical-sector beam continues scanning from broadside to forward endfire. This frequency-scanning concept for the two-sided pattern is illustrated in Fig. 1.

We specifically propose here a highly directive broadside, polarization-reconfigurable, pencil beam, by properly selecting an operating frequency near the splitting condition; i.e.,  $\beta_{-1} \approx \alpha$ , which corresponds to about 21.4 GHz [20.0 GHz] for  $\epsilon_r = 10.2$  [ $\epsilon_r = 11.5$ ]. By inspection of Fig. 2 a good leakage rate (i.e.,  $\alpha/k_0$  of the order of 0.05) is obtained when considering  $\epsilon_r = 11.5$ . Hence, we have selected an operating frequency of about 20 GHz for the practically realized and measured LWA structure. With this choice, to provide a radiation efficiency of about 90%, a radius for the antenna aperture equal to 8.5 cm was selected [1, Ch. 7].

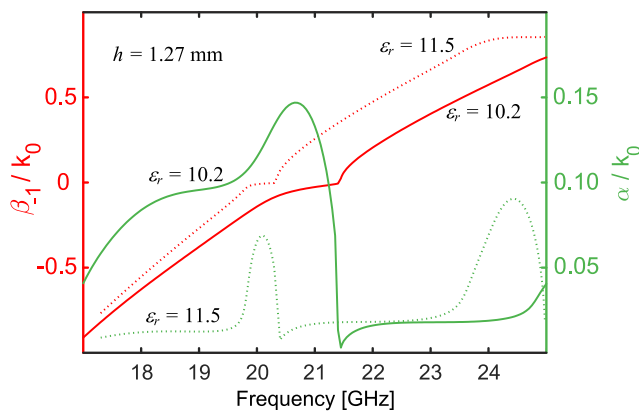


**FIGURE 2.** Normalized phase (left axis) and attenuation (right axis) constant of the TM LW mode for the considered MSG-GDS. Period and width of the metallic strip are  $d = 7$  mm and  $w = 1.25$  mm, respectively. Two relative dielectric constants are considered: solid [dashed] line  $\epsilon_r = 10.2$ [ $= 11.5$ ].

**B. SELECTION OF THE ANTENNA OPERATING STATE**

Once a commercially available GDS has been selected, the antenna operating state (AOS) for the LWA can be further studied [30], [31], which can enable optimal LW radiation from the guiding structure in the form of two-sided far-field patterns as well as a directive pencil beam at broadside. To support the description of the AOSs, Fig. 3 reports the corresponding Brillouin diagram for the structure in Fig. 2. The perturbed TM mode (black and gray lines) is shown with an open LW stopband at about 21.5 GHz. Also, the perturbed TE<sub>1</sub> mode can exist between about 20.8 GHz and 21.4 GHz when the TM mode is radiating, defining a suitable MSG-GDS configuration for one particular AOS.

By further analysis of the dispersive modes for the LWA, three distinct AOSs can be generally defined when antenna radiation is based on the leakage of the fundamental TM<sub>0</sub> SW mode [31]:

- AOS1: the TE<sub>1</sub> mode can radiate;
- AOS2: the TE<sub>1</sub> mode is bound;
- AOS3: the TE<sub>1</sub> SW mode is suppressed or cut-off.

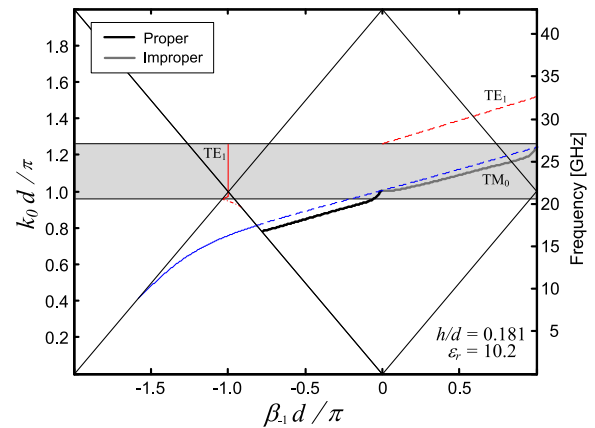


**FIGURE 3.** Brillouin diagram for the structure defined in Fig. 2 for  $\epsilon_r = 10.2$ . The blue solid and dashed lines represent the unperturbed mode.

As discussed in [31], AOS1 is considered to be unsuitable for efficient antenna operation since radiation can occur by both the TE<sub>1</sub> and TM<sub>0</sub> modes of the MSG-GDS. This can correspond to a multitude of leaky waves which can simultaneously radiate along the guiding surface. However, both AOS2 and AOS3 are suitable for the generation of broadside pencil beams in the far-field when efficient excitation of TM SWs is achieved by the feed system adopted here. In general, these AOSs are also frequency dependent and a LWA could start radiating in one operating state and enter into another with an increase in frequency. Given these possibilities for the different AOSs, and their dispersion behavior, careful attention is required during LWA design.

When examining the considered MSG of this paper, the TM<sub>0</sub> mode starts radiating at backward endfire by excitation of the  $n = -1$  space harmonic and the TE<sub>1</sub> mode is below cutoff, thus defining AOS3. For example, it can be observed in the dispersive diagram (see Fig. 3 with  $\epsilon_r = 10.2$ ,  $h = 1.27$  mm, and  $w/d = 0.179$ ,  $w$  being the width of the metallic strip) that the unperturbed (solid and dashed blue lines) [perturbed, solid black and gray lines] TM<sub>0</sub> mode indicates LW radiation above 17.41 GHz [16.75 GHz]. Below the cutoff of the perturbed TE<sub>1</sub> SW mode, its relevant phase constant is improper real, thus representing a nonphysical solution. This AOS defines an LWA which can support a two-sided conical pattern in the far field where the beam angle scans with frequency towards broadside; i.e.  $f < f_c$  as illustrated in Fig. 1. With an increase in frequency, the TE<sub>1</sub> mode can be supported by the MSG-GDS (between 20.81 GHz and 21.45 GHz), with broadside radiation made mainly possible by the dominantly excited TM<sub>0</sub> mode. This frequency range constitutes an MSG and LWA configuration offering AOS2, and we consider this suitable for our proposed design to ensure maximum realized gain at broadside.

Antenna operation in this frequency regime can be further understood by examining the reflection coefficient in Fig. 4 and when observing the far-field beam pattern for the proposed 2-D bull-eye configuration (see Fig. 5). Both consider

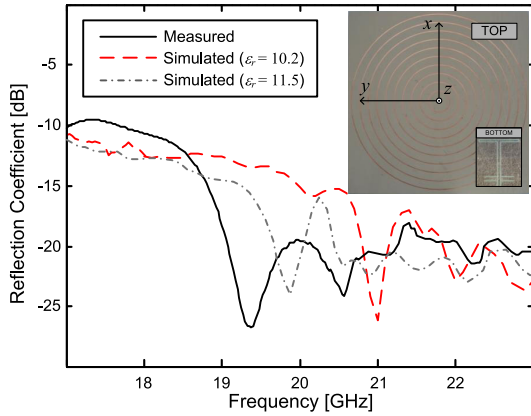


**FIGURE 4.** Reflection coefficient for the LWA structure with one non-directive SWL at the origin. Values are compared to full-wave simulations and a noticeable frequency shift is observed which is related to a practical tolerancing value for the relative dielectric constant of the employed GDS. A similar frequency shift (of about 1.5 GHz) was observed by the authors for the LWA presented in [31] which realized AOS3.

the basic case of a single non-directive SWL source placed at the origin (see Fig. 4 inset). Mainly due to the orientation of the individual SWL at the origin, this LWA can support two-sided frequency-beam scanning in the  $E(x-z)$  plane with sustained broadside radiation near  $f_c$  ( $\approx 20$  GHz) and conical-sector beam scanning with an increase in frequency.

This LWA grating topology (with  $w/d = 0.179$ ) allows for TE wave propagation when the  $TM_0$  SW mode is radiating which defines AOS2. Practically, this condition is realized by the MSG and the planar non-directive SWL which can generate TE field maximums in the  $\pm y$ -directions (along with the dominant TM fields in the  $\pm x$ -directions for LW radiation) [31], [37]. These TE waves are not suppressed, or reflected by the MSG, but supported in the noted passband regime (between 20.81 and 21.45 GHz, see Fig. 3). Consequently, reflection coefficient minimums can be reduced at the input at about 19.3 GHz for the measurements and about 21 GHz [20 GHz] as observed for the simulations which consider  $\epsilon_r = 10.2$  [ $\epsilon_r = 11.5$ ] in Fig. 4.

This downward frequency shift of about 1.5 GHz is consistent with previous findings [31] as well as the LW open-stopband frequency,  $f_c$  ( $\approx 20$  GHz) when considering  $\epsilon_r = 11.5$  (see Fig. 2). These matching conditions and the possibility of supporting TE fields in the form of microstrip ring modes of the “bull-eye” structure [31], help to facilitate a broadside beam maximum at about 20 GHz with gain values of more than 15 dB<sub>i</sub>. This can be observed in the measurements (see Fig. 15 from [31]) for the MSG with  $w/d = 0.179$  and with the single non-directive SWL. It should be mentioned that when considering other “bull-eye” configurations that suppress TE fields, i.e., belonging to AOS3, but with the azimuthal symmetry required here, similar realized gains were not observed; i.e., maximum values of only about 13 dB<sub>i</sub> were realized and with increased reflection loss values [31]. Given these findings, the design frequency of about 20 GHz and MSG-GDS configuration (with  $w/d = 0.179$  for AOS2)

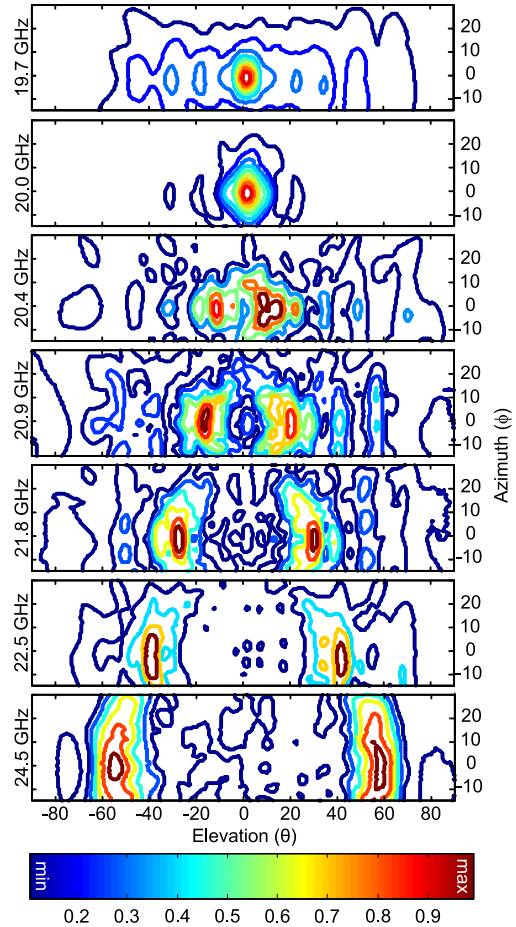


**FIGURE 5.** Measured 2-D beam patterns in the far-field with a single non-directive SWL at the structure origin (for  $h = 1.27$  mm and  $w/d = 0.179$  as in Fig. 2). High-quality two-sided beam scanning is observed as a function of frequency as well as a broadside pencil beam.

should be considered most suitable when requiring a LWA design with azimuthal symmetry and a directive pencil beam at broadside with maximum realized gain (about 15 dB<sub>i</sub>).

This 2-D LWA structure is investigated here using the four-port SWL source configuration. The fabricated antenna structure (see Fig. 11 in the following) as well as some details regarding full-wave simulations, CLW theory and measurements are outlined in the next sections. In particular, it is shown that, by properly exciting the four sources, by means of synthesis of a  $m = 0$  CLW, or, one or two  $m = 1$  CLWs, LP and CP patterns as well as sum and delta beams can flexibly be synthesized.

### III. RADIATION FEATURES

To accurately analyze the radiation features and the polarization diversity offered by the proposed LWA, we report here a full-wave numerical analysis of the array-fed LWA; they are performed with CST Microwave Studio exciting the structure with *ideal* horizontal magnetic monopoles placed on the ground plane. The structure parameters are as in Fig. 2 with the theoretical value for the permittivity of the GDS

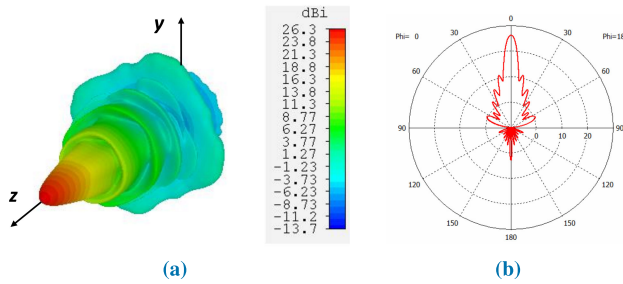


**FIGURE 6.** Simulated RHCP far-field pattern at  $f = 21.4$  GHz. (a) 3-D plot in dBi; (b) arbitrary azimuth cut.

(i.e.,  $\epsilon_r = 10.2$ ); one single frequency is analyzed, equal to  $f = 21.4$  GHz, which corresponds to broadside radiation for the considered LWA (see Fig. 2 for  $\epsilon_r = 10.2$ ).

Figure 6(a) reports a 3-D representation of the far-field patterns obtained by exciting the four ideal sources with the same amplitude and a phase progression from  $0^\circ$  to  $270^\circ$  (quadrature). A well-defined high-directional CP pencil beam, directed to broadside, is obtained. In fact the magnetic currents of the antipodal sources, that would be antiparallel with equiphased excitation, are here parallel thanks to their  $180^\circ$  electrical phase difference; hence, they radiate in-phase at broadside. The two antipodal pairs that constitute the array excite CLWs with a standing-wave azimuthal dependence of  $\cos(\phi)$  and  $\sin(\phi)$ , respectively. Also, since the two pairs are electrically in quadrature, their superposition is equivalent to a single CLW with a traveling wave having  $e^{\pm j\phi}$  azimuthal dependence that can generate a CP broadside far-field beam.

Since the pattern is azimuthally symmetric, an arbitrary azimuthal cut is reported in Fig. 6(b). The beam shows a maximum value for the directivity equal to 26 dBi, with a side-lobe level (SLL) below about 13 dBi, which is a standard value for non-tapered LWAs [1, Ch. 7]. We should mention that such a highly-directional beam is obtained with a *greatly reduced* number of elements with respect to the conventional free-space implementation of printed microstrip patches (some discussion on the *array thinning* concept can be found in [46]).

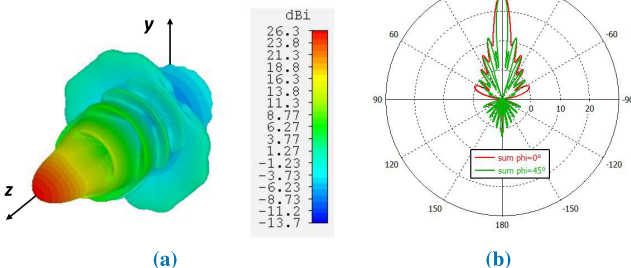


**FIGURE 7.** Simulated sum-beam pattern at  $f = 21.4$  GHz. (a) 3-D plot in dBi; (b) two azimuth cuts are reported:  $\phi = 0^\circ = 90^\circ$  and  $\phi = 45^\circ$ .

Figures 7 and 8 report a 3-D representation of the sum and delta far-field patterns, which enables the generation

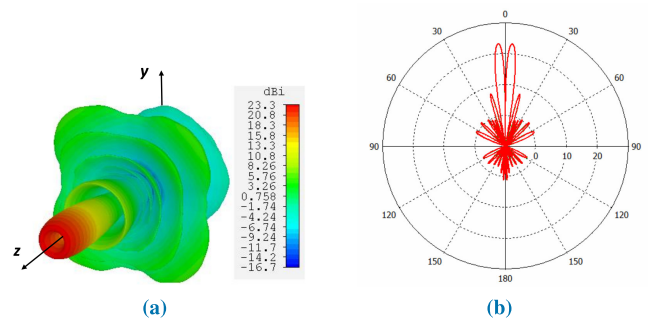


**FIGURE 8.** Simulated delta beam pattern at  $f = 21.4$  GHz. (a) 3-D plot in dBi; (b) arbitrary azimuth cut.

of highly directional beams for monopulse. Of course the antenna can operate by switching from one polarization state to the monopulse configuration by an external coupling circuit and/or feeding transmission lines of the required length, for example. The sum pattern (see Fig. 7) is obtained by enforcing an equi-amplitude excitation of the four sources and phasing from port 1 to port 4 as  $0^\circ, 0^\circ, 180^\circ, 180^\circ$  (or as  $0^\circ, 180^\circ, 180^\circ, 0^\circ$ ). Also in this case the two antipodal source pairs that constitute the array excite two CLWs with a standing-wave azimuthal dependence of  $\cos(\phi)$  and  $\sin(\phi)$ , respectively. However, now that such pairs are electrically in phase, their superposition is equivalent to a single CLW with a standing-wave  $\cos(\phi \pm \pi/4)$  dependence; this determines the asymmetric shape of the 3-D pattern (which is not azimuthally symmetric, see Fig. 7b). The delta pattern (see Fig. 8), instead, is obtained by enforcing equi-amplitude and equi-phase SW sources, thus exciting an azimuthally symmetric CLW. As expected, the delta beam presents a minimum at broadside (since, as already noted, any two antipodal sources will radiate out of phase at broadside) whereas the sum beam has a maximum at broadside; furthermore both cases show a good SLL, the highest sidelobe being more than 15 dB below the main-beam maximum.

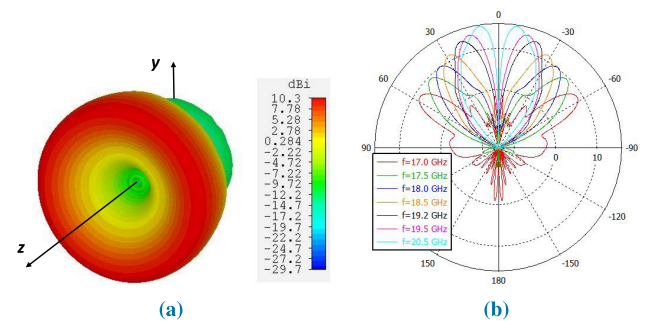


**FIGURE 9.** (a) Simulated conical pattern at  $f = 18$  GHz, 3-D plot in dBi; (b) scanning conical pattern for different frequency values (see legend).

It is also worth mentioning that, by means of an equi-amplitude and equi-phase excitation, the proposed LWA can also radiate a conical beam which scans with frequency [17], [33], [39]. This is achieved in the frequency region where  $|\beta_{-1}| \geq \alpha$ , and sustained leakage is provided by

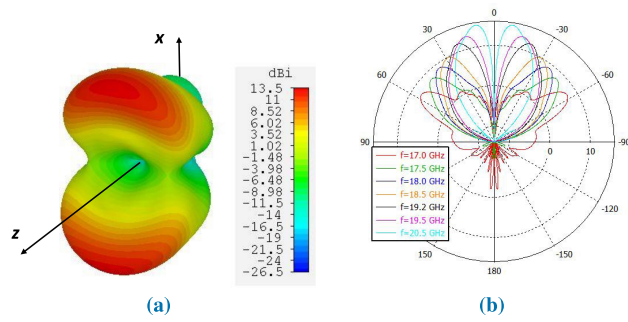


**FIGURE 10.** Simulated LP far-field pattern defining a conical-sector beam pattern that scans with frequency to broadside where ports 1 and 3 are driven with a 180° phase difference. (a) 3-D plot in dB; (b)  $\phi = 0^\circ$  azimuth cut of the scanning pattern for different frequencies.

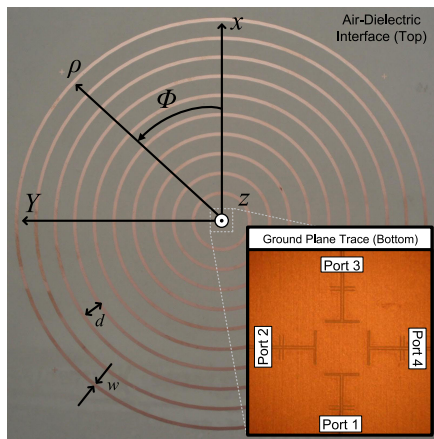


**FIGURE 11.** Fabricated and measured planar antenna defined by a MSG on a single-layer GDS with a 2 × 2 array of four SWLs placed at the origin for controlled field excitation on the aperture. The measured antenna prototype has 10 annular rings ( $w = 1.25$  mm and  $d = 7$  mm) defining the top radial aperture (similar to the MSG-GDS in the inset of Fig. 4).

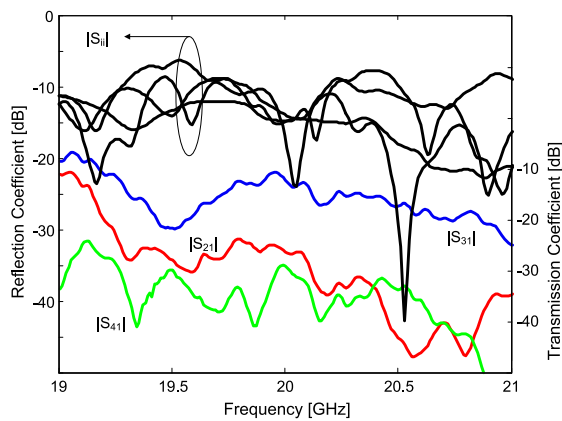


**FIGURE 12.** Measured reflection and transmission coefficients for the fabricated 4-port antenna structure in Fig. 11. At the design frequency of about 20 GHz all ports are matched with  $|S_{ii}|$  and port coupling well below 10 dB.

the LWA. Fig. 9(a) presents the conical scanning pattern at  $f = 18$  GHz, whereas Fig. 9(b) reports the scanning conical beam for different frequencies over an arbitrary

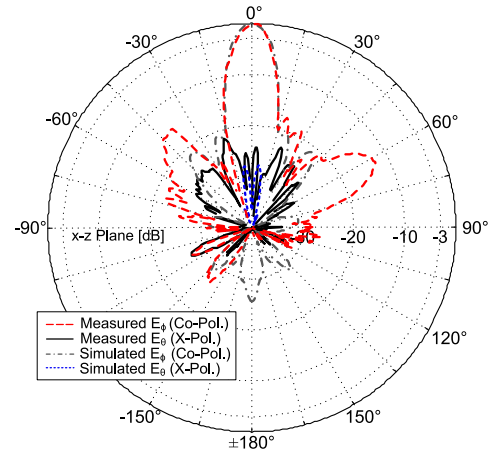


**FIGURE 13.** Measured and simulated LP beam pattern in the x-z plane at 19.9 GHz when Ports 1 and Ports 3 are driven.

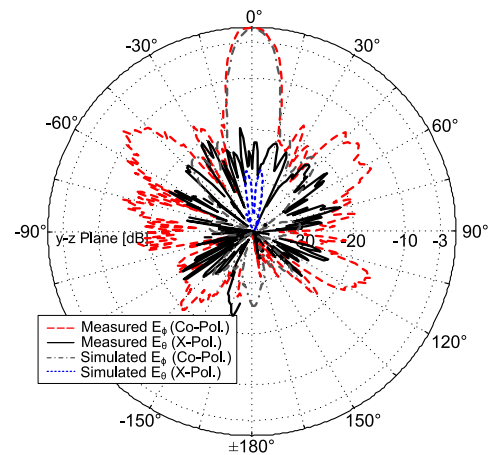


**FIGURE 14.** Measured and simulated LP beam pattern in the y-z plane at 19.9 GHz when Ports 2 and Ports 4 are driven.

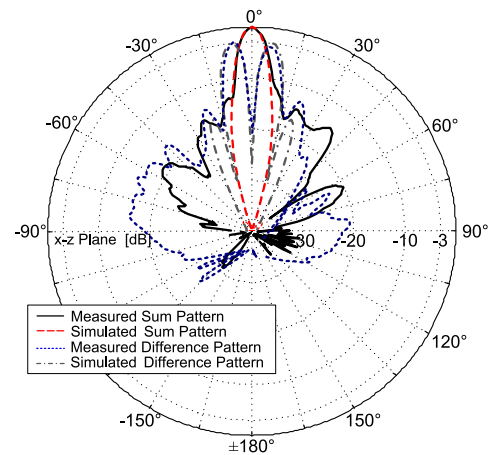


**FIGURE 15.** Comparison of the measured and simulated normalized sum and difference patterns at 19.9 GHz.

azimuthal cut. A two-sided (i.e., sector-like) conical pattern can also be achieved, as shown in Fig. 10, when ports 1 and 3 are driven (ports 2 and 4 are off) with a 180° phase difference, thus exciting a single CLW with a  $\sin \phi$  azimuthal dependence.

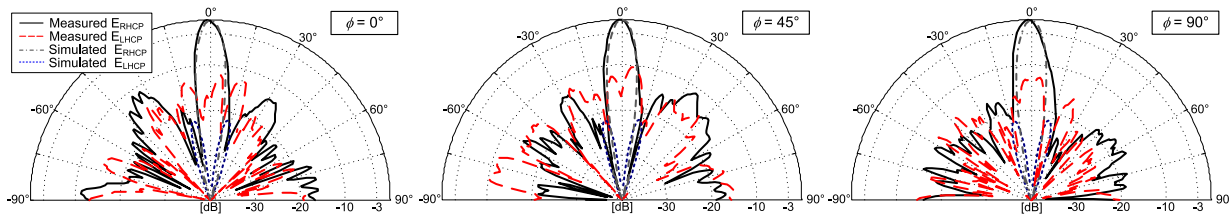


**FIGURE 16.** Measured CP beam patterns at 19.9 GHz for the MSG ‘bull-eye’ LWA shown in Fig. 11 by quadrature feeding of the SWLs. Directive beam patterns are observed at broadside with low cross-polarization levels (−10 dB). Observed gain values are also greater than 10 dB<sub>i</sub> at broadside.

**IV. EXPERIMENTAL RESULTS USING AN ARRAY OF SWLS**

In this section, we report the experimental characterization of the annular structure fed with a 2 × 2 non-directive SWL array as shown in Fig. 11. Measurements of the LP and CP as well as the delta and sum far-field beam patterns were performed in a calibrated anechoic chamber (see Figs. 12 - 19), while full-wave simulations of the complete structure were completed using a commercial solver (CST Microwave Studio). We emphasize that, during the measurements, networks of calibrated cables, power combiners, and external couplers were used to achieve the required relative phase difference between SWL elements.

To achieve the desired broadside pencil beam with polarization-reconfigurable features for the proposed 2-D LWA, the designed four-port SWL feed system can be suitably driven to generate the desired *m*-order CLW on the aperture. This is made possible by radiation of the relevant TM LW mode at about 20 GHz considering AOS2 for the designed MSG. If a uniform amplitude and constant phasing is considered, since both the structure and the feed excitation are azimuthally symmetric, the antenna radiates a dominant *m* = 0 CLW mode [38]. Conversely, by keeping constant the amplitude coefficients, and phasing the four SWLs (see inset in Fig. 1) with a progressive 90° phase between elements, two *m* = 1 CLWs (one in quadrature with respect to the other) can be generated and a far-field CP beam is obtained.

At the same time, once the structure has been designed to support a fast space harmonic (*n* = −1 in our case), whose complex wavenumber *k<sub>ρ</sub>* determines the propagation features of the CLW, the relative magnitude and phase of the elements within the feeding system, as well as the operational frequency, determine the shape and polarization of the far-field pattern realized by the LW fields excited on the aperture.

The employed SWL feed arrangement does not only offer the benefits of a single-layer structure and integrated coplanar waveguide feedline, but can also offer good reflection losses; i.e., |*S<sub>ii</sub>*| < −12 dB (where *i* is the *i*<sup>th</sup> port as shown in the inset of Fig. 12) with coupling values between ports less than about 15 dB at the 20 GHz design frequency. In addition, it should be mentioned that similar values were observed for the complete simulations for the structure (not shown for brevity). We should also mention that the |*S<sub>ii</sub>*| curves in Fig. 12 are not superimposed, as expected due to symmetry; this is mainly due to some very minor and

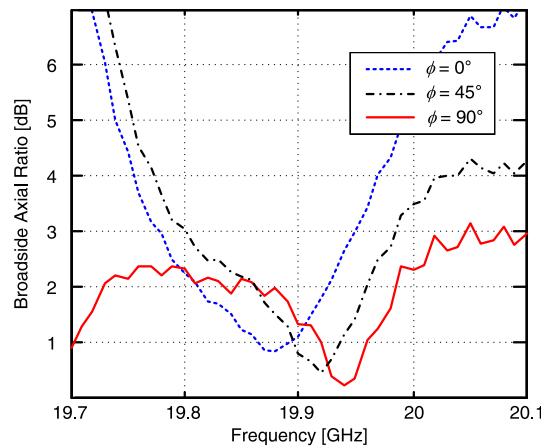


**FIGURE 17.** Measured axial ratio around the design frequency.

practical differences among the SWLs (due to fabrication) and to cables and devices used to perform the measurement.

Figure 13 reports the normalized patterns in the *x-z* plane by activating ports 1 and 3 and keeping the remaining two off. This excitation, having equi-amplitude and opposite phase, generates an LP pattern (defined by a single *m* = 1 CLW). The co-pol and cross-pol values are shown and a well-defined pencil beam can be observed for both the measurements and simulations (here and in the following, the latter are obtained tuning the value of the permittivity of the GDS, as discussed in Sect. II.A). Figure 14 reports the opposite case considering again the same amplitude coefficients for the ports 2 and 4, but with a 180° phase difference. The normalized LP pattern is reported in the *y-z* plane, and again, agreement between the simulated and measured broadside pencil beam is observed. In addition, Fig. 15 also reports a comparison among the measured and simulated sum and delta LP patterns obtained by driving the SWL as discussed in Sec. III. As expected, a slightly lower value (about 3 dB) is obtained for the delta pattern due to its conical nature.

Figures 16(a)-(c) report the RHCP measured pencil beam obtained by enforcing the following amplitude/phase configuration at each port: 1∠0°; 1∠90°; 1∠180°; 1∠270°, thus exciting two *m* = 1 CLWs. This quadrature feeding of the SWLs was achieved using external couplers (one 180° and two 90°) for the realization of a RHCP field distribution



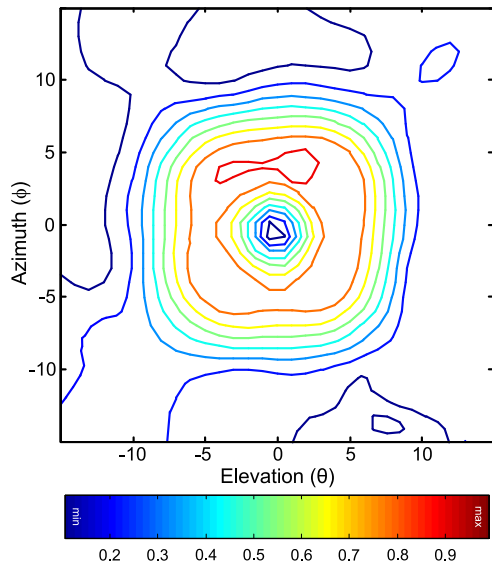


**FIGURE 18.** Measured 2-D difference pattern at 19.9 GHz (normalized and linear units), similar results for the sum pattern were observed as in Fig. 19. The unit of both axes are degrees.

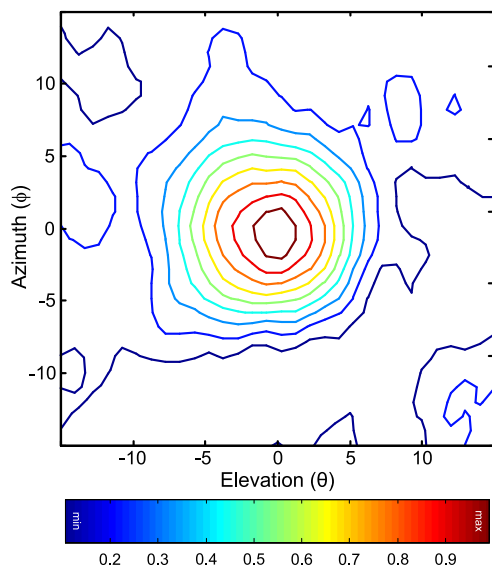


**FIGURE 19.** Measured 2-D RHCP beam pattern at 19.9 GHz. Results normalized to the observed maximum and shown in linear units. The unit of both axes are degrees.

on the aperture. A directive pattern is observed at broadside with max gain values greater than 10 dB<sub>i</sub>. The cross-polarization levels are well below 10 dB from the main maximum. The corresponding measured axial ratio is reported in Fig. 17 for three different azimuthal cuts (not superimposed due to practical tolerances), showing minimum values below 1 dB.

To better assess the diverse polarization performance of the proposed LWA, we also discuss the 2-D representation of the measured far-field patterns. For example, in Fig. 18 the 2-D measured delta pattern over the  $\phi$ - $\theta$  plane is shown.

The null of the pattern at broadside is clearly visible, thus generating a conical beam radiating off broadside. These results demonstrate that by controlling the relative phase and magnitude between the SWLs, it is possible to reconfigure the polarization state of the radiated beam and to generate patterns also for monopulse operation. Finally, Fig. 19 presents the measured 2-D RHCP pattern over the  $\phi$ - $\theta$  plane, confirming the pencil-beam nature of the CP radiation. A 3 dB radiating bandwidth at broadside of about 200 MHz has been achieved for the CP, sum/difference, and the one-sided beams, which is suitable for monopulse operation, as well as GPS and remote sensing applications. We also note that this bandwidth can be improved by shortening the antenna aperture and operating with a more relaxed beam-splitting condition, as numerically discussed in [47].

## V. CONCLUSION

A planar 2-D leaky-wave antenna providing a polarization-reconfigurable broadside pencil beam with high gain has been theoretically analyzed, designed, and measured. Leaky-wave theory has been exploited to determine the periodicity and the width of the relevant metal strip grating able to support directional radiation in the far field, as well as to characterize the role of the zeroth-order and the higher-order cylindrical leaky waves supported by the structure. The original  $2 \times 2$  array of SWLs, fully integrated within the ground plane of the proposed planar antenna, was also designed and discussed. The possibility of radiating, through the same design, linear and left/right circular polarization operation, as well as sum and delta beams for monopulse, has been demonstrated. Also, the measured and simulated results are in agreement and confirm the high quality of the circular polarized beams at broadside. The proposed 2-D planar leaky-wave antenna and 4-port surface-wave launcher feeding array may serve as a good candidate for next-generation of communication applications and other radar systems, which can greatly benefit from the availability of high-gain pencil beams with flexible control of the linear or circular polarization state.

## ACKNOWLEDGMENT

The authors would like to indicate that the work is only the authors views and that H2020 is not responsible for any information contained in the paper.

## REFERENCES

- [1] C. A. Balanis, *Modern Antenna Handbook*. Hoboken, NJ, USA: Wiley, 2011.
- [2] J. Huang, "A technique for an array to generate circular polarization with linearly polarized elements," *IEEE Trans. Antennas Propag.*, vol. AP-34, no. 9, pp. 1113–1124, Sep. 1986.
- [3] P. S. Hall, J. S. Dahele, and J. R. James, "Design principles of sequentially fed, wide bandwidth, circularly polarised microstrip antennas," *IEE Proc. H-Microw., Antennas Propag.*, vol. 136, no. 5, pp. 381–389, Oct. 1989.
- [4] A. Feresidis, K. Konstantinidis, and P. Gardner, "Fabry-Perot cavity antennas," in *Aperture Antennas for Millimeter and Sub-Millimeter Wave Applications*, A. Boriskin and R. Sauleau, Eds. Cham, Switzerland, 2018, ch. 7, pp. 325–367.

- [5] Z.-G. Liu and W.-B. Lu, "Low-profile design of broadband high gain circularly polarized Fabry-Perot resonator antenna and its array with linearly polarized feed," *IEEE Access*, vol. 5, pp. 7164–7172, 2017.
- [6] Z.-G. Liu, Z.-X. Cao, and L.-N. Wu, "Compact low-profile circularly polarized Fabry-Perot resonator antenna fed by linearly polarized microstrip patch," *IEEE Antennas Wireless Propag. Lett.*, vol. 15, pp. 524–527, 2016.
- [7] R. Orr, G. Goussetis, and V. Fusco, "Design method for circularly polarized Fabry-Perot cavity antennas," *IEEE Trans. Antennas Propag.*, vol. 62, no. 1, pp. 19–26, Jan. 2014.
- [8] S. A. Muhammad, R. Sauleau, and H. Legay, "Purely metallic waveguide-fed Fabry-Perot cavity antenna with a polarizing frequency selective surface for compact solutions in circular polarization," *IEEE Antennas Wireless Propag. Lett.*, vol. 11, pp. 881–884, 2012.
- [9] B. A. Zeb and K. P. Esselle, "High-gain dual-band dual-polarised electromagnetic band gap resonator antenna with an all-dielectric superstructure," *IET Microw. Antennas Propag.*, vol. 9, no. 10, pp. 1059–1065, 2015.
- [10] S. A. Muhammad, R. Sauleau, L. Le Coq, and H. Legay, "Self-generation of circular polarization using compact Fabry-Perot cavity antennas," *IEEE Antennas Wireless Propag. Lett.*, vol. 10, pp. 907–910, 2011.
- [11] D. R. Jackson and A. A. Oliner, "Leaky-wave antennas," in *Modern Antenna Handbook*, C. A. Balanis, Ed. Hoboken, NJ, USA, 2008, ch. 7, pp. 325–367.
- [12] T. Zhao, D. R. Jackson, and J. T. Williams, "2-D periodic leaky-wave antennas—Part II: Slot design," *IEEE Trans. Antennas Propag.*, vol. 53, no. 11, pp. 3515–3524, Nov. 2005.
- [13] Y.-L. Lyu, F.-Y. Meng, G.-H. Yang, D. Erni, Q. Wu, and K. Wu, "Periodic SIW leaky-wave antenna with large circularly polarized beam scanning range," *IEEE Antennas Wireless Propag. Lett.*, vol. 16, pp. 2493–2496, 2017.
- [14] H. Lee, J. H. Choi, C.-T. M. Wu, and T. Itoh, "A compact single radiator CRLH-inspired circularly polarized leaky-wave antenna based on substrate-integrated waveguide," *IEEE Trans. Antennas Propag.*, vol. 63, no. 10, pp. 4566–4572, Oct. 2015.
- [15] S. Otto, Z. Chen, A. Al-Bassam, A. Rennings, K. Solbach, and C. Caloz, "Circular polarization of periodic leaky-wave antennas with axial asymmetry: Theoretical proof and experimental demonstration," *IEEE Trans. Antennas Propag.*, vol. 62, no. 4, pp. 1817–1829, Apr. 2014.
- [16] J. L. Gómez-Tornero, D. Blanco, E. Rajo-Iglesias, and N. Llombart, "Holographic surface leaky-wave lenses with circularly-polarized focused near-fields—Part I: Concept, design and analysis theory," *IEEE Trans. Antennas Propag.*, vol. 61, no. 7, pp. 3475–3485, Jul. 2013.
- [17] D. Comite, P. Baccarelli, P. Burghignoli, and A. Galli, "Omnidirectional 2-D leaky-wave antennas with reconfigurable polarization," *IEEE Antennas Wireless Propag. Lett.*, vol. 16, pp. 2354–2357, 2017.
- [18] A. Al-Bassam, S. Otto, D. Heberling, and C. Caloz, "Broadside dual-channel orthogonal-polarization radiation using a double-asymmetric periodic leaky-wave antenna," *IEEE Trans. Antennas Propag.*, vol. 65, no. 6, pp. 2855–2864, Jun. 2017.
- [19] M. Sierra-Castañer, M. Sierra-Pérez, M. Vera-Isasa, and J. L. Fernández-Jambrina, "Low-cost monopulse radial line slot antenna," *IEEE Trans. Antennas Propag.*, vol. 51, no. 2, pp. 256–263, Feb. 2003.
- [20] A. Tamayo-Dominguez, J.-M. Fernandez-Gonzalez, and M. S. Castaner, "Low-cost millimeter-wave antenna with simultaneous sum and difference patterns for 5G point-to-point communications," *IEEE Commun. Mag.*, vol. 56, no. 7, pp. 28–34, Jul. 2018.
- [21] H. Wang, D.-G. Fang, and X. G. Chen, "A compact single layer monopulse microstrip antenna array," *IEEE Trans. Antennas Propag.*, vol. 54, no. 2, pp. 503–509, Feb. 2006.
- [22] Z.-C. Hao, H.-H. Wang, and W. Hong, "A novel planar reconfigurable monopulse antenna for indoor smart wireless access points' application," *IEEE Trans. Antennas Propag.*, vol. 64, no. 4, pp. 1250–1261, Apr. 2016.
- [23] H. Chu, J.-X. Chen, S. Luo, and Y.-X. Guo, "A millimeter-wave filtering monopulse antenna array based on substrate integrated waveguide technology," *IEEE Trans. Antennas Propag.*, vol. 64, no. 1, pp. 316–321, Jan. 2016.
- [24] Z.-G. Liu and Y.-X. Guo, "Monopulse Fabry-Perot resonator antenna," in *Proc. Int. Symp. Antennas Propag. (ISAP)*, vol. 2, Oct. 2013, pp. 664–667.
- [25] G. Minatti, F. Caminita, M. Casaletti, and S. Maci, "Spiral leaky-wave antennas based on modulated surface impedance," *IEEE Trans. Antennas Propag.*, vol. 59, no. 12, pp. 4436–4444, Dec. 2011.
- [26] A. Vosoogh, A. Haddadi, A. U. Zaman, J. Yang, H. Zirath, and A. A. Kishk, "W-band low-profile monopulse slot array antenna based on gap waveguide corporate-feed network," *IEEE Trans. Antennas Propag.*, vol. 66, no. 12, pp. 6997–7009, Dec. 2018.
- [27] S. K. Podilchak, A. P. Freundorfer, and Y. M. M. Antar, "A new configuration of printed non-directive surface-wave sources for advanced beam control," in *Proc. 14th Int. Symp. Antenna Technol. Appl. Electromagn. Amer. Electromagn. Conf. (ANTEM-AMEREM)*, Jul. 2010, pp. 1–4.
- [28] S. K. Podilchak, A. P. Freundorfer, and Y. M. M. Antar, "Multilayer antennas for directive beam steering broadside radiation and circular polarization," in *Proc. 4th Eur. Conf. Antennas Propag.*, Apr. 2010, pp. 1–5.
- [29] D. Comite *et al.*, "Analysis and design of a circularly-polarized planar leaky-wave antenna," in *Proc. IEEE Int. Symp. Antennas Propag.*, Jul. 2018, pp. 2133–2134.
- [30] P. Baccarelli, P. Burghignoli, G. Lovat, and S. Paulotto, "A novel printed leaky-wave 'bull-eye' antenna with suppressed surface-wave excitation," in *Proc. IEEE Int. Symp. Antennas Propag.*, vol. 1, Jun. 2004, pp. 1078–1081.
- [31] S. K. Podilchak, P. Baccarelli, P. Burghignoli, A. P. Freundorfer, and Y. M. M. Antar, "Analysis and design of annular microstrip-based planar periodic leaky-wave antennas," *IEEE Trans. Antennas Propag.*, vol. 62, no. 6, pp. 2978–2991, Jun. 2014.
- [32] U. Beaskoetxea *et al.*, "77-GHz high-gain bull's-eye antenna with sinusoidal profile," *IEEE Antennas Wireless Propag. Lett.*, vol. 14, pp. 205–208, 2015.
- [33] D. Comite *et al.*, "Planar antenna design for omnidirectional conical radiation through cylindrical leaky waves," *IEEE Antennas Wireless Propag. Lett.*, vol. 17, no. 10, pp. 1837–1841, Oct. 2018.
- [34] S. F. Mahmoud, Y. M. M. Antar, H. F. Hammad, and A. P. Freundorfer, "Theoretical considerations in the optimization of surface waves on a planar structure," *IEEE Trans. Antennas Propag.*, vol. 52, no. 8, pp. 2057–2063, Aug. 2004.
- [35] S. K. Podilchak, A. P. Freundorfer, and Y. M. M. Antar, "Surface-wave launchers for beam steering and application to planar leaky-wave antennas," *IEEE Trans. Antennas Propag.*, vol. 57, no. 2, pp. 355–363, Feb. 2009.
- [36] M. Ettore, S. Bruni, G. Gerini, A. Neto, N. Llombart, and S. Maci, "Sector PCS-EBG antenna for low-cost high-directivity applications," *IEEE Antennas Wireless Propag. Lett.*, vol. 6, pp. 537–539, 2007.
- [37] S. K. Podilchak, "Planar leaky-wave antennas Microw. Circuits by practical Surf. Wave launching," Ph.D. dissertation, Queen's Univ., Kingston, ON, Canada, 2013.
- [38] A. Ip and D. R. Jackson, "Radiation from cylindrical leaky waves," *IEEE Trans. Antennas Propag.*, vol. 38, no. 4, pp. 482–488, Apr. 1990.
- [39] C. A. Allen, C. Caloz, and T. Itoh, "Leaky-waves in a metamaterial-based two-dimensional structure for a conical beam antenna application," in *IEEE MTT-S Int. Microw. Symp. Dig.*, vol. 1, Jun. 2004, pp. 305–308.
- [40] P. C. Dubois-Fernandez, J. C. Souyris, S. Angelliaume, and F. Garestier, "The compact polarimetry alternative for spaceborne SAR at low frequency," *IEEE Trans. Geosci. Remote Sens.*, vol. 46, no. 10, pp. 3208–3222, Oct. 2008.
- [41] P. Baccarelli *et al.*, "Full-wave analysis of printed leaky-wave phased arrays," *Int. J. RF Microw. Comput.-Aided Eng.*, vol. 12, no. 3, pp. 272–287, 2002.
- [42] P. Baccarelli *et al.*, "Modal properties of surface and leaky waves propagating at arbitrary angles along a metal strip grating on a grounded slab," *IEEE Trans. Antennas Propag.*, vol. 53, no. 1, pp. 36–46, Jan. 2005.
- [43] D. Comite *et al.*, "A dual-layer planar leaky-wave antenna designed for linear scanning through broadside," *IEEE Antennas Wireless Propag. Lett.*, vol. 16, pp. 1106–1110, 2017.
- [44] D. Comite *et al.*, "Radially periodic leaky-wave antenna for Bessel beam generation over a wide-frequency range," *IEEE Trans. Antennas Propag.*, vol. 66, no. 6, pp. 2828–2843, Jun. 2018.
- [45] G. Lovat, P. Burghignoli, and D. R. Jackson, "Fundamental properties and optimization of broadside radiation from uniform leaky-wave antennas," *IEEE Trans. Antennas Propag.*, vol. 54, no. 5, pp. 1442–1452, May 2006.
- [46] R. Gardelli, M. Albani, and F. Capolino, "Array thinning by using antennas in a Fabry-Perot cavity for gain enhancement," *IEEE Trans. Antennas Propag.*, vol. 54, no. 7, pp. 1979–1990, Jul. 2006.
- [47] A. Sutinjo, M. Okoniewski, and R. H. Johnston, "Beam-splitting condition in a broadside symmetric leaky-wave antenna of finite length," *IEEE Antennas Wireless Propag. Lett.*, vol. 7, pp. 609–612, 2008.



**DAVIDE COMITE** (M'15) received the master's degree (*cum laude*) in telecommunications engineering and the Ph.D. degree in electromagnetics and mathematical models for engineering from the Sapienza University of Rome, Rome, Italy, in 2011 and 2015, respectively, where he is currently a Postdoctoral Researcher.

He was a Visiting Ph.D. student with the Institute of Electronics and Telecommunications of Rennes, University of Rennes 1, France, in 2014, and a Postdoctoral Researcher with the Center of Advanced Communications, Villanova University, PA, USA, in 2015. His scientific interests include the design of dual-polarized leaky-wave antennas, 2-D periodic leaky-wave antennas, and the generation of non-diffracting waves and pulses. He is also interested in the study of the scattering from natural surfaces and the characterization of the GNSS reflectometry over the land. His activity also regards microwave imaging and objects detection and the modeling of the radar signature in forward scatter radar systems.

Dr. Comite was a recipient of the Marconi Junior Prize assigned by Fondazione Guglielmo Marconi, to a young student author of a master's degree thesis, particularly relevant and important in information and communications technology, in 2012, the Minerva Award 2017, assigned by the Sapienza University of Rome and Fondazione Sapienza to Postdoctoral Researchers who developed distinguished research activities. In 2017, he was a finalist of the Best Paper Award, Electromagnetics and Antenna Theory Section, at the 11th European Conference on Antennas and Propagation. He was a co-author of the Best Student Paper Award at the SPIE Remote Sensing and Security+Defence International Symposia, in 2017, and a recipient of the Best Paper Award, Electromagnetics and Antenna Theory Section, at the 12th European Conference on Antennas and Propagation, in 2018, and the Barzilai Prize for the best scientific work of under-35 researchers at the National Meeting of Electromagnetics (XXII RiNem), in 2018. He is currently an Associate Editor of the IEEE ACCESS, the *IET Journal of Engineering*, and the *IET Microwaves, Antennas & Propagation*.



**SYMON K. PODILCHAK** received the B.A.Sc. degree in engineering science from the University of Toronto, ON, Canada, in 2005, the M.A.Sc. degree in electrical engineering from the Royal Military College of Canada, Kingston, ON, Canada, in 2008, and the Ph.D. degree in electrical engineering from Queen's University, Kingston, in 2013, where he received the Outstanding Dissertation Award for his Ph.D. degree.

From 2013 to 2015, he was an Assistant Professor with Queen's University. He then joined Heriot-Watt University, Edinburgh, U.K., in 2015, as an Assistant Professor and became an Associate Professor, in 2017. His research is supported by the H2020 Marie Skłodowska-Curie European Research Fellowship and cross-appointed at The University of Edinburgh, U.K. He is a registered Professional Engineer (P.Eng.), has had industrial experience as a Computer Programmer, and has designed 24- and 77-GHz automotive radar systems with Samsung and Magna Electronics. His recent industry experience also includes the design of high-frequency surface-wave radar systems, and professional software design and implementation for measurements in anechoic chambers for the Canadian Department of National Defence and the SLOWPOKE Nuclear Reactor Facility. He has also designed new compact multiple-input multiple-output antennas for wideband military communications, highly compact circularly polarized antennas for microsatellites with COM DEV International, and new wireless power transmission systems for Samsung. His research interests include surface waves, leaky wave antennas, metasurfaces, UWB antennas, phased arrays, and CMOS integrated circuits.

Dr. Podilchak was a recipient of many best paper awards and scholarships; most notably Research Fellowships from the IEEE Antennas and Propagation Society and the IEEE Microwave Theory and Techniques Society. He also received a Postgraduate Fellowship from the Natural Sciences and Engineering Research Council of Canada and four Young Scientist Awards from the International Union of Radio Science. In 2011 and 2013, he received Student Paper Awards from the IEEE International Symposium on Antennas and Propagation, and the Best Paper Prize for Antenna Design from the European Conference on Antennas and Propagation for his work on CubeSat antennas, in 2012, and The European Microwave Prize for his research on surface waves and leaky wave antennas, in 2016. In 2017, he was bestowed the Visiting Professorship Award at Sapienza University of Rome. In 2014, he was recognized as an Outstanding Reviewer for the IEEE TRANSACTIONS ON ANTENNAS AND PROPAGATION by the IEEE Antennas and Propagation Society. He was also the Founder and first Chairman of the IEEE Antennas and Propagation Society and the IEEE Microwave Theory and Techniques Society, and Joint Chapter of the IEEE Kingston Section in Canada. In recognition of these services, the IEEE presented him with the Outstanding Volunteer Award, in 2015. He currently serves as an Associate Editor for the *IET Electronic Letters*.



**PAOLO BACCARELLI** (M'01) received the Laurea degree in electronic engineering and the Ph.D. degree in applied electromagnetics from the Sapienza University of Rome, Rome, Italy, in 1996 and 2000, respectively, where he joined the Department of Electronic Engineering, in 1996, and has been an Assistant Professor, since 2010.

He was a Visiting Researcher with the University of Houston, Houston, TX, USA, in 1999. In 2017, he joined the Department of Engineering, Roma Tre University, Rome, where he has been an Associate Professor, since 2017. In 2017, he received the National Scientific Qualification for the role of Full Professor of electromagnetic fields in Italian Universities. He has co-authored about 230 papers in international journals, conference proceedings, and book chapters. His research interests include the analysis and design of planar antennas and arrays, leakage phenomena in uniform and periodic structures, numerical methods for integral equations and periodic structures, propagation and radiation in anisotropic media, metamaterials, graphene, and electromagnetic band-gap structures.

Dr. Baccarelli was a recipient of the Giorgio Barzilai Laurea Prize presented by the former IEEE Central and South Italy Section, from 1994 to 1995. He serves on the editorial board of international journals and acts as a Reviewer for more than 20 IEEE, IET, OSA, and AGU journals. He was a Secretary of the 2009-European Microwave Week and has been a member of the TPCs of several international conferences.



**PAOLO BURGHIGNOLI** (S'97–M'01–SM'08) was born in Rome, Italy, in 1973. He received the Laurea degree (*cum laude*) in electronic engineering and the Ph.D. degree in applied electromagnetics from the Sapienza University of Rome, Rome, in 1997 and 2001, respectively, where he joined the Electronic Engineering Department (now Department of Information Engineering, Electronics and Telecommunications), in 1997.

He was a Visiting Research Assistant Professor with the University of Houston, Houston, TX, USA, in 2004. From 2010 to 2015, he was an Assistant Professor with the Sapienza University of Rome, where he has been an Associate Professor, since 2015. In 2017, he received the National Scientific Qualification for the role of Full Professor of electromagnetic fields in Italian Universities. He has co-authored “Fast Breaking Papers, October 2007” in EE and CS, about metamaterials (paper that had the highest percentage increase in citations in Essential Science Indicators). His scientific interests include analysis and design of planar antennas and arrays, leakage phenomena in uniform and periodic structures, numerical methods for integral equations and periodic structures, propagation and radiation in metamaterials, electromagnetic shielding, and graphene electromagnetics.

Dr. Burghignoli was a recipient of the Giorgio Barzilai Laurea Prize presented by the former IEEE Central & South Italy Section, from 1996 to 1997, the 2003 IEEE MTT-S Graduate Fellowship, and the 2005 Raj Mittra Travel Grant for Junior Researchers presented at the IEEE AP-S Symposium on Antennas and Propagation, Washington, DC, USA. He is an Associate Editor of the *IET Electronics Letters* and the *Hindawi International Journal of Antennas and Propagation*.



**ALESSANDRO GALLI** (S'91–M'96) received the Laurea degree in electronic engineering and the Ph.D. degree in applied electromagnetics from the Sapienza University of Rome, Italy, in 1990 and 1994, respectively, where he has been with the Department of Electronic Engineering (now Department of Information Engineering, Electronics, and Telecommunications), since 1990.

He became an Assistant Professor and an Associate Professor with the Sapienza University of Rome, in 2000 and 2002, respectively. He passed the National Scientific Qualification as a Full Professor in the sector of electromagnetics, in 2013. He is currently teaching the courses of “electromagnetic fields,” “antennas and propagation,” and “engineering electromagnetics” for electronics and communications engineering at the Sapienza University of Rome. He has authored more than 300 papers on journals, books, and conferences. He holds a patent for an invention concerning a type of microwave antenna. His research interests include theoretical and applied electromagnetics, mainly focused on modeling, numerical analysis, and design for antennas and passive devices from microwaves to terahertz: specific topics involve leaky waves, periodic and multilayered printed structures, metamaterials, and graphene, and other topics of interest involve geoelectromagnetics, bioelectromagnetics, and microwave plasma heating for alternative energy sources.

Dr. Galli is a member of the European School of Antennas. He is also a member of the leading scientific societies of electromagnetics. He was a recipient of various grants and prizes for his research activity: the Barzilai Prize for the best scientific work of under-35 researchers at the 10th National Meeting of Electromagnetics, in 1994, and the Quality Presentation Recognition Award at the International Microwave Symposium by the Microwave Theory and Techniques Society of the Institute of Electrical and Electronics Engineering, in 1994 and 1995. He was elected as the Italian Representative of the Board of Directors of the European Microwave Association, the main European Society of Electromagnetics, for the 2010–2012 triennium and then re-elected for the 2013–2015 triennium. He was the General Co-Chair of the European Microwave Week, the most important conference event in the electromagnetic area at European level in 2014. Since its foundation in 2012, he has been the Coordinator of the European Courses on Microwaves, the first European educational institution on microwaves. He was an Associate Editor of the *International Journal of Microwave and Wireless Technologies* (Cambridge University Press) and the *IET Microwaves, Antennas & Propagation* (Institution of Engineering and Technology).



**ALOIS P. FREUNDORFER** (SM'90) received the B.A.Sc., M.A.Sc., and Ph.D. degrees from the University of Toronto, Toronto, ON, Canada, in 1981, 1983, and 1989, respectively. In 1990, he joined the Department of Electrical Engineering, Queen's University, Kingston, ON. Since 1990, he has been involved in the nonlinear optics of organic crystals, coherent optical network analysis, and microwave integrated circuits. He was involved in high speed IC design for use in lightwave systems with bit

rates in excess of 40 Gb/s and in millimeter wave integrated circuits used in wireless communications. His current research interests include growing 3-D low temperature ceramics on ICs and printed circuit boards with applications to sensors and low power tunable circuits.



**YAHIA M. M. ANTAR** (S'73–M'76–SM'85–LF'00) received the B.Sc. degree (Hons.) from Alexandria University, Alexandria, Egypt, in 1966, and the M.Sc. and Ph.D. degrees from the University of Manitoba, MB, Canada, in 1971 and 1975, respectively, all in electrical engineering. In 1977, he held a Government of Canada Visiting Fellowship with the Communications Research Centre, Ottawa. In 1979, he joined the Division of Electrical Engineering, National Research Council

of Canada. In 1987, he joined the Department of Electrical and Computer Engineering, Royal Military College of Canada, Kingston, where he has been a Professor, since 1990. He has authored or co-authored over 200 journal papers, several books, and chapters in books, over 450 refereed conference papers, holds several patents, has chaired several national and international conferences, and has given plenary talks at many conferences. He has supervised and co-supervised over 90 Ph.D. and M.Sc. theses at the Royal Military College of Canada and at Queens University, several of which have received the Governor General of Canada Gold Medal Award, the Outstanding Ph.D. Thesis of the Division of Applied Science, and many best paper awards in major international symposia. He is a Fellow of the Engineering Institute of Canada, the Electromagnetic Academy, and the International Union of Radio Science. He served as the Chair of CNC, URSI (1999–2008), and Commission B (1993–1999), and has a cross appointment at Queen's University, Kingston. He serves as an Associate Editor of many IEEE and IET journals and as an IEEE-APS Distinguished Lecturer. In 2002, he was awarded a Tier 1 Canada Research Chair in electromagnetic engineering, which has been renewed in 2016. In 2003, he was awarded the Royal Military College of Canada Excellence in Research Prize, and the RMCC Class of 1965 Teaching Excellence Award, in 2012. He was elected by the URSI to the Board as the Vice President, in 2008 and 2014, and by the IEEE AP AdCom., in 2009. He was appointed as a member of the Canadian Defence Advisory Board of the Canadian Department of National Defence, in 2011. In 2012, he received the Queens Diamond Jubilee Medal from the Governor General of Canada in recognition for his contribution to Canada. He was a recipient of the 2014 IEEE Canada RA Fessenden Silver Medal for Ground Breaking Contributions to Electromagnetics and Communications, and the 2015 IEEE Canada J. M. Ham outstanding Engineering Education Award. In 2015, he received the Royal Military College of Canada Cowan Prize for excellence in research. He was a recipient of the IEEE-AP-S the Chen-To-Tai Distinguished Educator Award, in 2017.

...